

End-to-end Kernel Learning via Generative Random Fourier Features

Kun Fang^a, Xiaolin Huang^{a,*}, Fanghui Liu^b, Jie Yang^{a,*}

^a*Institute of Image Processing and Pattern Recognition, Institute of Medical Robotics,
Shanghai Jiao Tong University, Shanghai 200240, P.R. China*

^b*Department of Electrical Engineering (ESAT-STADIUS), KU Leuven, B-3001 Leuven,
Belgium*

Abstract

Random Fourier features enable researchers to build feature map to learn the spectral distribution of the underlying kernel. Current distribution-based methods follow a two-stage scheme: they first learn and optimize the feature map by solving the kernel alignment problem, then learn a linear classifier on the features. However, since the ideal kernel in kernel alignment problem is not necessarily optimal in classification tasks, the generalization performance of the random features learned in this two-stage manner can perhaps be further improved. To address this issue, we propose an end-to-end, one-stage kernel learning approach, called generative random Fourier features, which jointly learns the features and the classifier. A generative network is involved to implicitly learn and to sample from the distribution of the latent kernel. Random features are then built via the generative weights and followed by a linear classifier parameterized as a full-connected layer. We jointly train the generative network and the classifier by solving the empirical risk minimization problem for a one-stage solution. Straightly minimizing the loss between predictive and true labels brings better generalization performance. Besides, this end-to-end strategy allows us to increase the depth of features, resulting in multi-layer architecture and exhibiting strong linear-separable pattern. Empirical results demonstrate

*Corresponding authors.

Email addresses: fanghenshao@sjtu.edu.cn (Kun Fang), xiaolinhuang@sjtu.edu.cn (Xiaolin Huang), lfhsagre@outlook.com (Fanghui Liu), jieyang@sjtu.edu.cn (Jie Yang)

the superiority of our method in classification tasks over other two-stage kernel learning methods. Finally, we investigate the robustness of proposed method in defending adversarial attacks, which shows that the randomization and re-sampling mechanism associated with the learned distribution can alleviate the performance decrease brought by adversarial examples.

Keywords: generative random Fourier features, end-to-end, one-stage, multi-layer, adversarial attack

1. Introduction

Kernel methods reveal non-linear property hidden in data and have been extensively studied in recent decades [1, 2]. The selection of kernel still remains a non-trivial problem, which requires prior knowledge and directly affects the algorithm performance. Hence, various methods are devoted to learn a kernel function or a kernel matrix from data, such as multiple kernel learning [3, 4], deep kernel learning [5, 6], and non-parametric kernel learning [7]. Despite the great performance these methods have achieved, there still exist some limitations among them. For example, the parametric form in function learning limits the flexibility, and the learned matrix encounters the problem of no straightforward extensions for out-of-sample data points. To address these issues, another type of kernel learning approaches propose to learn and optimize explicit feature maps, which map input points into a new high-dimensional space, to approximate the kernel by modeling the distribution of kernel [8, 9, 10]. These approaches are based on the Bochner’s theorem [11], which indicates that the Fourier transform of a kernel function is associated to a probability distribution: A continuous, shift-invariant kernel $k(\mathbf{x}, \mathbf{x}') = k(\mathbf{x} - \mathbf{x}')$ on \mathcal{R}^d is positive definite if and only if $k(\cdot)$ is the Fourier transform of a non-negative measure $p(\mathbf{w})$. That is,

$$k(\mathbf{x} - \mathbf{x}') = \int_{\mathcal{R}^d} p(\mathbf{w}) e^{j\mathbf{w}^T(\mathbf{x} - \mathbf{x}')} d\mathbf{w}. \quad (1)$$

Therefore, by randomly sampling a group of weights $\{\mathbf{w}_i\}_{i=1}^D$ from the spectral distribution of kernel (Fourier transform of kernel), one can first construct an

explicit feature map,

$$\phi(\mathbf{x}, \{\mathbf{w}_i\}_{i=1}^D) \equiv \sqrt{\frac{1}{D}} [\cos(\mathbf{w}_1^T \mathbf{x}) \cdots \cos(\mathbf{w}_D^T \mathbf{x}) \sin(\mathbf{w}_1^T \mathbf{x}) \cdots \sin(\mathbf{w}_D^T \mathbf{x})]^T, \quad (2)$$

known as the random Fourier features (RFF), then obtain a linear classifier on these features to categorize them. From this point of view, learning the spectral distribution of kernel by constructing the RFF is an alternative choice to learn a positive definite, shift-invariant kernel [8].

To involve data information, typical approaches [9, 10] propose to solve the following kernel alignment problem [12] to learn the random features,

$$\arg \max_{\mathbf{w}} \mathbb{E}_{(\mathbf{x}, y), (\mathbf{x}', y')} yy' \phi(\mathbf{x}, \mathbf{w})^T \phi(\mathbf{x}', \mathbf{w}), \quad (3)$$

where (\mathbf{x}, y) and (\mathbf{x}', y') denote a pair of training samples and the inner product of the two mapped points $\phi(\mathbf{x}, \mathbf{w})^T \phi(\mathbf{x}', \mathbf{w})$ denotes the implicit kernel function values $k(\mathbf{x}, \mathbf{x}')$. [9] selects an optimal weight subset from $\{\mathbf{w}_i\}_{i=1}^D$ by solving Eq.(3), and thus constructs an optimal feature subset based on the vanilla RFF and proves the consistency and generalization bound, which is efficient and highly scalable. [10] incorporates a deep neural network to implicitly learn the spectral distribution of kernel, and trains the network by solving Eq.(3), which shows that the performance could be improved by involving a network to model the spectral distribution of kernel.

These kernel learning methods [9, 10] follow a *two-stage* scheme: They first learn and optimize the random features by solving Eq.(3), and then learn a linear classifier on the features. The optimization target of Eq.(3) is to learn a suitable kernel via kernel alignment to approximate the ideal kernel $\mathbf{y}\mathbf{y}^T$. However, the ideal kernel is not necessarily optimal in the view of classification. Hence, in such a two-stage way, the random features learned in the first stage does not take much care of the generalization or classification performance, which could be further improved.

To address this issue, we propose to jointly learn the random features and classifier in an end-to-end way by straightly solving the expectation risk mini-

mization problem,

$$\arg \min_{G, C} \mathbb{E}_{(\mathbf{x}, y)} [L(C[\phi(\mathbf{x}, \mathbb{E}_{\mathbf{n}}[G(\mathbf{n})]]), y)], \quad (4)$$

where $L(\cdot, \cdot)$ denotes the loss function and \mathbf{n} denotes the noise variable. A generative network $G(\cdot)$ is involved to learn the distribution of kernel, which takes a group of noise as input and performs as a *sampler*. Then, generative RFF is constructed based on the weights sampled from the learned distribution. A linear classifier $C(\cdot)$ parameterized as a full-connected (FC) layer is applied to the generative RFF to categorize them. The generative network and the linear classifier are jointly trained by directly minimizing the loss between the predicted labels and the true labels. Therefore, we achieve an end-to-end, *one-stage* solution, which no longer pursues the approximation ability of the random features. Instead, it is expected that distributions of the underlying kernel can be modeled by the generative network for better classification or generalization performance.

Further, this end-to-end training strategy allows us to go deeper and deeper. That is, with one generator, we can build the first layer of random features of original data. Then, with another generator, a second layer of random features can be constructed in the same way based on the features in the previous layer. After such a layer-by-layer abstraction, the random features in the last layer are followed with an FC layer. The total networks, i.e., the generators in all layers and the last full-connected layer, are again jointly trained to solving Eq.(4). In this way, in each layer of features, there is a corresponding generator which models the specific distribution on this layer of features. Hence the random features in the last layer exhibit strong linear-separable pattern. In two-stage approaches [8, 9, 10], the distribution is learned by the guide of an ideal kernel, which is restricted to a *single-layer* structure, since the guiding kernel for multi-layer is not clear. While we cover the *multi-layer* case and have an advantage in recognizing data pattern. One problem brought by the multi-layer structure is the training of multiple generative networks. Directly updating the parameters in these generators perhaps results in a total failure of convergence. Hence we

design a progressive training strategy to efficiently train the generators in each layer in an inverse, layer-by-layer order.

In short, by involving multiple generative networks and adopting the end-to-end training strategy, the proposed method could learn the implicit distribution of the underlying kernel and shows superior classification performance. Besides, knowing the distribution of the parameters makes it possible to resample and obtain randomness. On the one hand, the proposed method can output stable results, which is based on that different resampling noises still produce similar accuracies, and on the other hand, the randomness is helpful for adversarial robustness. Extensive experiment results demonstrate not only the performance improvements in classification tasks compared with other two-stage, RFF-based methods, but also the robustness in defending adversarial attacks.

Our contributions can be summarized as follows,

- To the best of our knowledge, this is the first work for an end-to-end, one-stage method, which implicitly learns some latent distributions of kernel via generative models and random Fourier features. Empirical results indicate the superiority of our method over other two-stage, RFF-based methods in classification tasks.
- The end-to-end strategy enables us to employ a multi-layer structure for generative RFF, which means a good kernel on features. The performance of multi-layer structure are better than that of single-layer structure. In addition, we design a progressive training strategy to efficiently train the generators in different layers.
- The robustness of proposed method in adversarial attacks is also investigated. Empirical results show that, to some degree, the randomization and resampling mechanism associated with the learned distributions can alleviate the performance decrease brought by adversarial examples.

The rest of this paper is organized as follows. We briefly introduce the random Fourier features and generative models in Section 2. The one-stage framework,

multi-layer architecture, and progressive training strategy of proposed method are explained in Section 3. Experiment results on classification tasks and adversarial attacks are shown in Section 4 and the discussions and conclusions are drawn in Section 5.

2. Preliminaries

2.1. Random Fourier Features

In kernel methods, a positive definite kernel $k(\mathbf{x}, \mathbf{x}')$ with $\mathbf{x}, \mathbf{x}' \in \mathcal{R}^d$ defines a map $\Phi : \mathcal{R}^d \rightarrow \mathcal{H}$, which satisfies $k(\mathbf{x}, \mathbf{x}') = \langle \Phi(\mathbf{x}), \Phi(\mathbf{x}') \rangle_{\mathcal{H}}$, where $\langle \cdot, \cdot \rangle_{\mathcal{H}}$ denotes the inner product in a Reproducing Kernel Hilbert Space \mathcal{H} . However, in large-scale kernel machines, there exist unacceptable high computation and memory costs: $\mathcal{O}(n^2)$ kernel evaluations, $\mathcal{O}(n^2)$ in space, and even $\mathcal{O}(n^3)$ in time to compute the inverse of kernel matrix. Therefore, randomized features are introduced to approximate the kernel function [8]. The theoretical foundation is based on the Bochner's theorem.

According to Bochner's theorem, considering real-valued, shift-invariant, and positive definite kernel, by applying Euler's formula $e^{jx} = \cos(x) + j \sin(x)$ to Eq.(1), we have

$$k(\mathbf{x} - \mathbf{x}') = \text{Re}[k(\mathbf{x} - \mathbf{x}')] = \int_{\mathcal{R}^d} p(\mathbf{w}) \cos(\mathbf{w}^T(\mathbf{x} - \mathbf{x}')) d\mathbf{w}. \quad (5)$$

Next, by the standard trigonometric identity $\cos(a-b) = \cos(a)\cos(b) + \sin(a)\sin(b)$, we have

$$\begin{aligned} & \int_{\mathcal{R}^d} p(\mathbf{w}) \cos(\mathbf{w}^T(\mathbf{x} - \mathbf{x}')) d\mathbf{w} \\ &= \int_{\mathcal{R}^d} p(\mathbf{w}) (\cos(\mathbf{w}^T \mathbf{x}) \cos(\mathbf{w}^T \mathbf{x}') + \sin(\mathbf{w}^T \mathbf{x}) \sin(\mathbf{w}^T \mathbf{x}')) d\mathbf{w} \\ &= \mathbb{E}_{\mathbf{w}} [[\cos(\mathbf{w}^T \mathbf{x}), \sin(\mathbf{w}^T \mathbf{x})]^T [\cos(\mathbf{w}^T \mathbf{x}'), \sin(\mathbf{w}^T \mathbf{x}')]]. \end{aligned} \quad (6)$$

Therefore, one can construct an explicit feature map $\phi : \mathcal{R}^d \rightarrow \mathcal{R}^{2D}$ defined in Eq.(2) by sampling a group of weights $\{\mathbf{w}_i\}_{i=1}^D$ from the spectral distribution of the kernel function. Hence it could be observed that tuning the weight parameters is equal to learning the distribution. The mapped random Fourier features

satisfy $\phi(\mathbf{x}, \{\mathbf{w}_i\}_{i=1}^D)^T \phi(\mathbf{x}', \{\mathbf{w}_i\}_{i=1}^D) \approx k(\mathbf{x}, \mathbf{x}')$ [8]. A detailed analysis of the convergence can be found in [13].

RFF facilitates kernel methods a lot in large-scale tasks and has also been utilized in other domains. [14] proposes a fast surrogate leverage weighted sampling strategy to generate refined random Fourier features. [15] proposes a new extreme learning method based on the RFF of original data. [16] rethinks the traditional bias-variance trade-off in machine learning with the help of RFF.

In vanilla RFF, Bochner’s theorem guarantees the convergence of RFF by sampling from the spectral distribution of kernel, which indicates that learning distribution is equal to learning the kernel. Hence, to efficiently learn the distribution, the generative model is introduced.

2.2. Generative Models

Generative models have been widely applied in learning distributions from data [17]. Various generative models can be categorized into two types: models that perform explicit probability density estimation and models that perform as a *sampler* sampling from specific distribution without a precise probability function.

Suppose a training set includes samples from a distribution \mathbb{P}_{data} , and the first type of generative models returns an estimation \mathbb{P}_{model} of \mathbb{P}_{data} . Given a particular value as input, \mathbb{P}_{model} will output the corresponding probability. While the second type tries to learn the latent \mathbb{P}_{data} as well, but in a rather different way: The learned model actually simulates a sampling process, through which one can create more samples from the estimated distribution.

There exist lots of researches in the second type of generative models using neural network as the sampler. In computer vision, the family of generative adversarial networks (GANs) [18] has shown great generality in multiple situations, including unsupervised learning [19] and high-resolution image generation [20]. The generative network in GAN performs as a useful image distribution generator, which is able to generate verisimilar images. Besides, in bayesian deep learning, there is a series of hypernetwork-based work, which uses a neural

network, called hypernet, to generate the parameters in another neural network, called primary net. The hypernet also performs as a sampler to learn the parameter posterior distribution of primary net [21, 22].

By involving generative networks, on the one hand, the proposed method is able to learn a good distribution from data, which means a good kernel. On the other hand, the proposed method could resample different parameters from the learned distribution via the generative network, bringing the latent advantage of robustness under adversarial attacks.

3. Generative Random Fourier Features Model

3.1. One-stage Generative Random Fourier Features

Previous RFF-based kernel learning methods construct random features via sampling from the spectral distribution of the kernel or via approximating the ideal kernel, and then train a classifier on these features. The classification performance of the random features learned in this two-stage manner can perhaps be further improved. Therefore, we propose generative RFF to jointly learn the features and the classifier by optimizing the expectation risk minimization problem in an end-to-end manner, which leads to a one-stage solution with better classification performance.

We first describe a general framework of our one-stage model, illustrated in Fig.1: A generator is designed to learn and to sample from the latent distribution of kernel, then, the generative random Fourier features (GRFF) of original data are constructed by the weights sampled from the generative distribution. Finally, a linear classifier is applied to the features to categorize them.

The generator in our method performs as a *sampler*. It implicitly learns some distribution \mathbb{P}_k and generates samples from it. Given an arbitrary noise distribution \mathbb{P}_0 and a group of noises $\mathbf{N} = \{\mathbf{n}_i\}_{i=1}^D$ sampled from \mathbb{P}_0 , the generator Φ_G takes them as input and generates a group of weights $\{\mathbf{w}_i\}_{i=1}^D$ sampled from \mathbb{P}_k :

$$\mathbf{w}_i = \Phi_G(\mathbf{n}_i), \mathbf{n}_i \sim \mathbb{P}_0, \mathbf{w}_i \sim \mathbb{P}_k, i = 1, \dots, D. \quad (7)$$

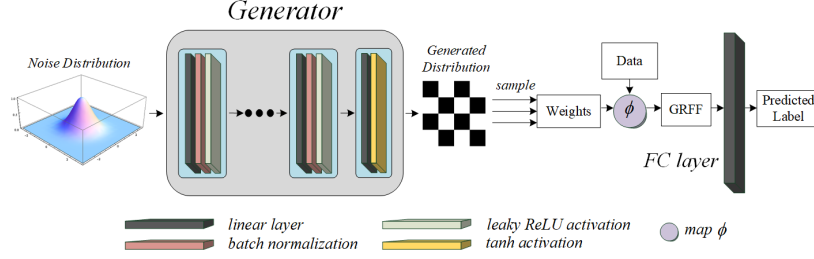


Figure 1: Illustration of the one-stage generative random Fourier features.

Given a training set $\{(\mathbf{x}_i, y_i)\}_{i=1}^n \subset \mathcal{R}^d \times \{0, 1\}$, the generative random Fourier features \mathbf{z}_i of each training point \mathbf{x}_i will be constructed with full use of the D weights according to Eq.(2):

$$\mathbf{z}_i = \phi(\mathbf{x}_i, \{\mathbf{w}_j\}_{j=1}^D), \mathbf{w}_j \sim \mathbb{P}_k, i = 1, \dots, n. \quad (8)$$

Notice that \mathbf{w}_j and \mathbf{x}_i are of the same dimension and that the dimension of \mathbf{z}_i equals to $2D$. Finally, the linear classifier Φ_C will be applied on the GRFF $\{\mathbf{z}_i\}_{i=1}^n$ to predict labels $\hat{y}_i = \Phi_C(\mathbf{z}_i)$.

Denote θ_G and θ_C as the parameters of generator Φ_G and linear classifier Φ_C respectively. Combining Eq.(7) and Eq.(8), we have the following empirical risk minimization (ERM) problem:

$$\min_{\theta_G, \theta_C} \frac{1}{n} \sum_{i=1}^n L(\Phi_C(\phi[\mathbf{x}_i, \Phi_G(\mathbf{N})]), y_i). \quad (9)$$

3.2. Multi-layer Generative Random Fourier Features

The end-to-end training strategy by straightly optimizing the ERM problem naturally allows us to employ a multi-layer structure of the generative RFF, which is shown in Fig.2.

Take the simplest two-layer structure as example. Denote Φ_{G_1} and Φ_{G_2} as the two generators in the first and second layer respectively. Φ_{G_1} and Φ_{G_2} take different groups of noise $\mathbf{N}_1 = \{\mathbf{n}_i^1\}_{i=1}^{D_1}$ and $\mathbf{N}_2 = \{\mathbf{n}_i^2\}_{i=1}^{D_2}$ sampled from the same distribution \mathbb{P}_0 as input respectively, and generate corresponding weights

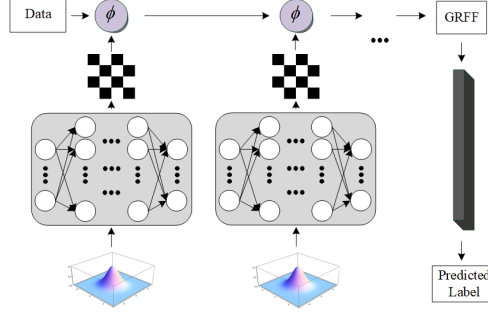


Figure 2: Illustration of the generative RFF with multi-layer architecture.

$\mathbf{W}_1 = \{\mathbf{w}_i^1\}_{i=1}^{D_1}$ and $\mathbf{W}_2 = \{\mathbf{w}_i^2\}_{i=1}^{D_2}$:

$$\begin{aligned}\mathbf{w}_i^1 &= \Phi_{G_1}(\mathbf{n}_i^1), \mathbf{n}_i^1 \sim \mathbb{P}_0, \mathbf{w}_i^1 \sim \mathbb{P}_{k_1}, i = 1, \dots, D_1, \\ \mathbf{w}_i^2 &= \Phi_{G_2}(\mathbf{n}_i^2), \mathbf{n}_i^2 \sim \mathbb{P}_0, \mathbf{w}_i^2 \sim \mathbb{P}_{k_2}, i = 1, \dots, D_2,\end{aligned}\tag{10}$$

where \mathbb{P}_{k_1} and \mathbb{P}_{k_2} are the distributions modeled by Φ_{G_1} and Φ_{G_2} respectively.

In the first layer, the training samples $\{\mathbf{x}_i\}_{i=1}^n$ are cooperated together with \mathbf{W}_1 to construct the generative RFF in this layer $\mathbf{Z}_1 = \{\mathbf{z}_i^1\}_{i=1}^n$ according to Eq.(2):

$$\mathbf{z}_i^1 = \phi(\mathbf{x}_i, \{\mathbf{w}_j^1\}_{j=1}^{D_1}), \mathbf{w}_j^1 \sim \mathbb{P}_{k_1}, i = 1, \dots, n.\tag{11}$$

Then, \mathbf{Z}_1 are cooperated together with the generative weights \mathbf{W}_2 from the second layer to construct the generative RFF in the second layer $\mathbf{Z}_2 = \{\mathbf{z}_i^2\}_{i=1}^n$ in the same way:

$$\mathbf{z}_i^2 = \phi(\mathbf{z}_i^1, \{\mathbf{w}_j^2\}_{j=1}^{D_2}), \mathbf{w}_j^2 \sim \mathbb{P}_{k_2}, i = 1, \dots, n.\tag{12}$$

Again, notice that \mathbf{w}_j^1 and \mathbf{x}_i are of the same dimension and that the dimension of \mathbf{z}_i^1 equals to $2D_1$. Therefore, the dimension of \mathbf{w}_j^2 must equal to $2D_1$ and the dimension of \mathbf{z}_i^2 equals to $2D_2$. Finally, there is a linear classifier Φ_C applied to the last GRFF \mathbf{Z}_2 to predict labels.

Now we rewrite the ERM problem in Eq.(9) for two-layer GRFF as follows,

$$\min_{\theta_{G_1}, \theta_{G_2}, \theta_C} \frac{1}{n} \sum_{i=1}^n L(\Phi_C(\phi[\mathbf{z}_i^1, \Phi_{G_2}(\mathbf{N}_2)]), y_i), \mathbf{z}_i^1 = \phi[\mathbf{x}_i, \Phi_{G_1}(\mathbf{N}_1)].\tag{13}$$

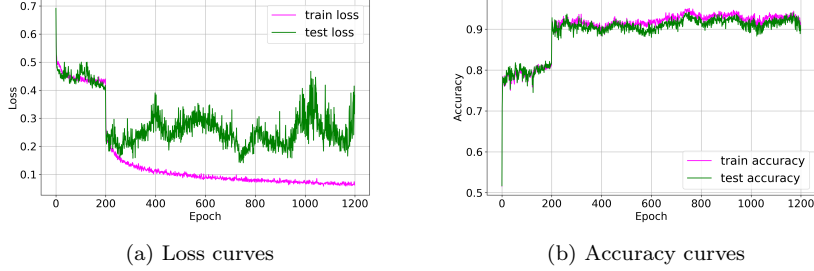


Figure 3: An example of the training process on a bi-classification task. A two-layer architecture is adopted. Loss and accuracy variations are recorded. There are evident performance leaps, i.e., the drop of losses and the step-up of accuracies, by adding a second layer at the turning point of 200-th epoch. Detailed settings about this example can be found in section 4.

Advantages of the multi-layer structure are obvious. The generator in current layer actually models some distribution on the features in previous layer, which means a good kernel on the features. Besides, associated with the proposed progressive training strategy (introduced in section 3.3), during the whole training process, by updating the generators layer-by-layer, there are distinct improvements on both the loss curves and the accuracy curves, which can be referred to Fig.3 and indicates significant performance leaps by adding more layers. More details about the distribution on features are illustrated in the experiment section.

3.3. Progressively Training

For multi-layer generative random Fourier features, since there are several generative networks, it is hard to efficiently update all the parameters in different networks simultaneously, which possibly results in a total failure of convergence. To efficiently train the multiple generative networks, inspired by the training strategy in ProGAN [20], we propose a similar progressive, layer-by-layer training strategy.

The progressive training strategy contains several stages. The number of stages equals to the number of generators. In the first stage, we freeze the

update of all the parameters except the last generator and the FC layer. In the second stage, we unfreeze the second to the last generator and update it with the last generator and FC layer while keep the others fixed. In such an inverse, layer-by-layer order, we progressively unfreeze the generators in each layer, add them to the training sequence one by one, and finally train all these generators together with the FC layer, which is an efficient training way for the multi-layer structure. The training algorithm for a two-layer structure is demonstrated in Alg.1.

In addition, there are some other details. Every generator is parameterized by a multi-layer perceptron (MLP) containing several blocks. Each block holds a linear layer, a batch normalization [23] layer, and an activation layer except for the last one. We cancel the batch normalization layer and set *tanh* function as the activation function in the last block and leaky ReLU in the others. The detailed components of each part are also shown in Fig.1. One can customize the structure details according to the specific cases. For example, it is free to add linear layers or neurons to the MLP to enhance its learning ability or to add dropout [24] to prevent it from overfitting. Besides, The number of neurons in the last full-connected layer can be modified freely such that it can also be applied in multi-classification or regression tasks.

The standard normal distribution is set as the input noise distribution, which corresponds to an RBF kernel, the most widely used universal kernel. At each iteration, we *re-sample* a group of noises from \mathbb{P}_0 to optimize the generator on the expectation of distribution, and update *simultaneously* the parameters of the generator and the classifier by Adam [25] optimizer. We choose the cross entropy function as the loss function L . One can estimate whether the model is trained perfectly by watching the variation of the cross entropy loss value, with which the final classification performance is closely connected.

For the inference process, given a new sample \mathbf{x}_{new} , random noises are first sampled from \mathbb{P}_0 , then weights are generated via generators, then corresponding generative random Fourier features \mathbf{z}_{new} are constructed via weights and \mathbf{x}_{new} by applying Eq.(8) or Eq.(11), Eq.(12). Finally, the linear classifier Φ_C will

predict the label of \mathbf{x}_{new} .

Algorithm 1 Progressively Training for GRFF with Two-layer Architecture

Require: Training set $X_{tr} = \{(\mathbf{x}_i, y_i)\}_{i=1}^n$, learning rates η_1 and η_2 for the first and second stage respectively, numbers of training epochs $epoch_1$ and $epoch_2$ for the first and second stage respectively, batch size b .

Ensure: Generators Φ_{G_1} and Φ_{G_2} , a linear classifier Φ_C .

- 1: **while** not reach $epoch_1 + epoch_2$ **do**
 - 2: Sample $\mathbf{N}_1 = \{\mathbf{n}_i^1\}_{i=1}^{D_1}$ and $\mathbf{N}_2 = \{\mathbf{n}_j^2\}_{j=1}^{D_2}$, each $\mathbf{n}_i^1 \sim \mathbb{P}_0, \mathbf{n}_j^2 \sim \mathbb{P}_0$.
 - 3: Take a batch of samples $\{\mathbf{x}_i, y_i\}_{i=1}^b \subseteq X_{tr}$.
 - 4: Compute the batch loss: $\frac{1}{b} \sum_{i=1}^b L(\Phi_C\{\phi[\mathbf{z}_i^1, \Phi_{G_2}\{\mathbf{N}_2\}]\}, y_i)$,
 where $\mathbf{z}_i^1 = \phi[\mathbf{x}_i, \Phi_{G_1}\{\mathbf{N}_1\}]$.
 - 5: **if** not reach $epoch_1$ **then**
 - 6: Compute the gradients: $g_{G_2} = \nabla_{\theta_{G_2}} loss, g_C = \nabla_{\theta_C} loss$.
 - 7: Update θ_{G_2} and θ_C at k -th iteration simultaneously by
 $\theta_{G_2}^{(k+1)} = \theta_{G_2}^{(k)} - \eta_1 Adam(\theta_{G_2}^{(k)}, g_{G_2}), \theta_C^{(k+1)} = \theta_C^{(k)} - \eta_1 Adam(\theta_C^{(k)}, g_C)$.
 - 8: **else if** not reach $epoch_1 + epoch_2$ **then**
 - 9: Compute the gradients:
 $g_{G_1} = \nabla_{\theta_{G_1}} loss, g_{G_2} = \nabla_{\theta_{G_2}} loss, g_C = \nabla_{\theta_C} loss$.
 - 10: Update $\theta_{G_1}, \theta_{G_2}$ and θ_C at k -th iteration simultaneously by
 $\theta_{G_1}^{(k+1)} = \theta_{G_1}^{(k)} - \eta_2 Adam(\theta_{G_1}^{(k)}, g_{G_1}), \theta_{G_2}^{(k+1)} = \theta_{G_2}^{(k)} - \eta_2 Adam(\theta_{G_2}^{(k)}, g_{G_2}),$
 $\theta_C^{(k+1)} = \theta_C^{(k)} - \eta_2 Adam(\theta_C^{(k)}, g_C)$.
 - 11: **end if**
 - 12: **end while**
-

So far, we finish building an end-to-end, one-stage kernel learning method, which implicitly learns the distribution of kernel by solving an ERM problem via generative random Fourier features. To learn the latent distribution of kernel, a generative network is designed to simulate the sampling process without an explicit definition of the probability density function of the distribution. Besides, jointly learning the features and classifier allows us to increase the depth of the features. The multi-layer architecture can learn a good kernel on features

and thus bring performance improvements. In addition, a progressive training strategy is proposed to efficiently train the multiple generative networks.

4. Experiments and Results

We evaluate the classification performance of the proposed generative RFF on a wide range of data sets. Following the work in [9, 10], we first test the performance on a synthetic data set. Second, we choose several benchmark data sets from the UCI repository¹ and LIBSVM data², including both large-scale sets and small-scale sets, and test the performance on these data sets. Finally, we introduce the variant of multi-layer GRFF for image data and conduct an adversarial attack on this variant to illustrate its robustness. All the experiments are executed on a workstation with a single NVIDIA GPU GTX 1070.

The simplest version of the generative RFF only includes a single layer, i.e., one single generative network, denoted as SL-GRFF. We denote multi-layer generative RFF including more than one generators as ML-GRFF. We compare SL-GRFF and ML-GRFF with the following approaches.

- RFF [8]. [8] first proposes the vanilla random Fourier features to approximate kernel functions by sampling from the spectral distribution of kernel functions, which is a data-independent approach.
- OPT-RFF [9]. Based on the vanilla RFF, [9] proposes to optimize the features by solving a kernel alignment problem. [9] selects a feature subset in an optimal size, which shows great superiority in high processing speed in large-scale kernel machines.
- IKL [10]. [10] adopts a neural network to model the spectral distribution of kernel function. The network is trained by optimizing a kernel alignment problem. A linear classifier is then applied on the features.

¹<https://archive.ics.uci.edu/ml/datasets.html>

²<https://www.csie.ntu.edu.tw/~cjlin/libsvmtools/datasets/>

- MLP. We compare ML-GRFF with traditional multi-layer perceptron (MLP) with ReLU activation function. The number of the neurons in each hidden layer of the MLP equals to the number of sampled noise in each layer of ML-GRFF.

In all the experiments, for RFF and OPT-RFF, we set radial basis function (RBF) kernel as its kernel function. The ridge regression is set as the linear classifier in the second stage of RFF and OPT-RFF. A large enough number of features are initialized in OPT-RFF to automatically select a feature subset of an optimal size for every data set. The optimal number of features will then be adopted in RFF. We only compare with the results of IKL claimed in the paper [10] on the synthetic data set.

For our proposed method, in section 4.1 and 4.2, for the multi-layer version, we adopt a two-layer generative RFF including two generators, each of which is parameterized by an MLP. We set $D_1 = 256$ and $D_2 = 64$. The structures of the first and second generator are $100 \rightarrow 128 \rightarrow 64 \rightarrow 64 \rightarrow \dim$ and $100 \rightarrow 512 \rightarrow 256 \rightarrow 256 \rightarrow 512$ respectively, where \dim denotes the dimension of the input data. The FC layer contains 128 neurons. For the single-layer generative RFF in section 4.1, the generator is also parameterized as an MLP and holds a structure of $100 \rightarrow 128 \rightarrow 64 \rightarrow 64 \rightarrow \dim$. We set $D = 256$, thus the FC layer in single-layer structure contains 512 neurons.

4.1. Performance on Synthetic Data

In this synthetic set, we generate data $\{\mathbf{x}_i\}_{i=1}^n \sim \mathcal{N}(0, I_d)$ with $y_i = \text{sign}(\|\mathbf{x}_i\|^2 - \sqrt{d})$, where d is data dimension. The training set includes 10^4 samples and test set contains 10^3 samples. Fig.4a shows the data distribution when $d = 2$. One can find that Gaussian kernel (RBF kernel) is ill-suited for this data set [9].

Fig.4b illustrates the test errors of different methods corresponding to different data dimensions $d \in \{2, 4, 6, 8, \dots, 18, 20\}$. Both RFF and OPT-RFF manifest a sharp performance degradation along with the increase of d . On the other hand, IKL and ML-GRFF both have rather stable performance with the variation of dimensions since they try to learn distribution of kernel via a

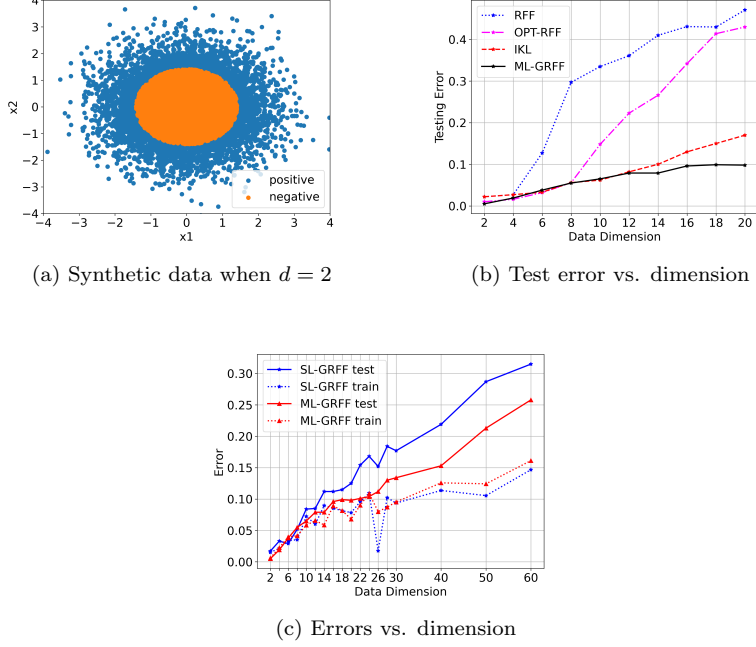


Figure 4: Performance on synthetic data. (a) Data distribution when dimension equals to 2. (b) Misclassification errors on test set of different methods. (c) Misclassification errors on training and test sets of generative RFF with single-layer architecture and multi-layer architecture.

generative network without any prior kernel function definition. Particularly, by directly optimizing the ERM problem in an end-to-end manner, ML-GRFF characterizes the data pattern much better than the others and achieves the lowest test errors.

Fig.4c shows the comparison results on the training and test sets between the generative RFF with single-layer architecture and multi-layer architecture. In a wider range of the data dimension, ML-GRFF always has an evident superiority of the classification errors on test set over SL-GRFF.

Besides, to visualize the generative RFF, we take PCA [26] to extract the top-3 principal components of the features in SL-GRFF and different layers of ML-GRFF, which are shown in Fig.5. We choose two different dimensions,

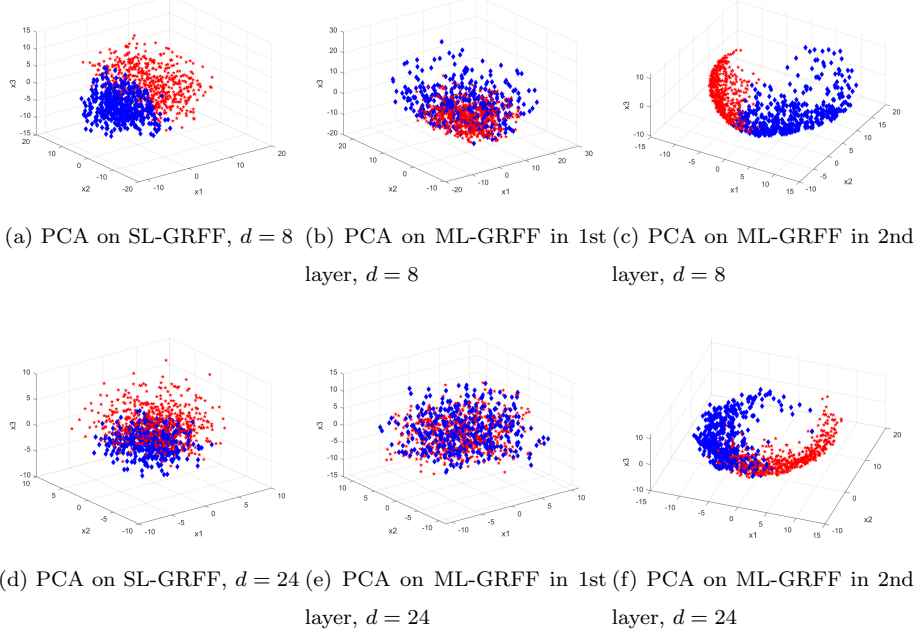
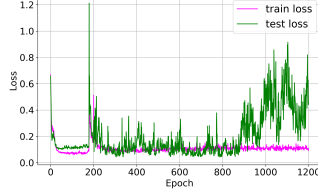


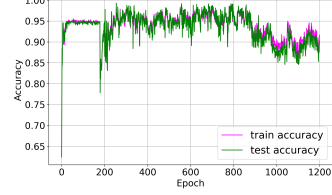
Figure 5: Visualization of the PCA results on the SL-GRFF and different layers in ML-GRFF, corresponding to synthetic data when $d = 8$ and $d = 24$ respectively. The blue diamond points denote positive samples, while the red pentagram points denote negative samples.

$d = 8$ and $d = 24$. When $d = 8$, both SL-GRFF and ML-GRFF have similar performance, while when $d = 24$, ML-GRFF performs better than SL-GRFF. For ML-GRFF, the extracted principal components in the 1st layer in Fig.5b and Fig.5e do not show any evident linear separability. But, in Fig.5c and Fig.5f, the components in the 2nd layer follow a clear linear separable distribution. For SL-GRFF, we can also see linear separability of the extracted components from Fig.5a and Fig.5d, which is obviously weaker than that of the extracted components of the 2nd layer in ML-GRFF. Hence, by going deeper and deeper, ML-GRFF is able to learn a good kernel on features, which results in better performance.

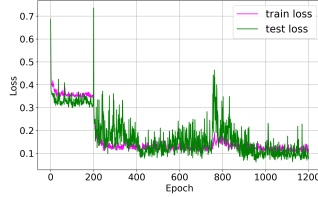
To illustrate the traits of the progressive training strategy, we record the loss and accuracy curves during training for synthetic data of different dimensions



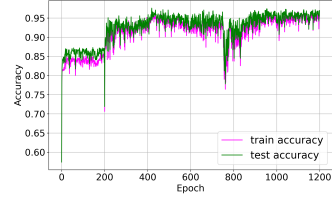
(a) Loss curves when $d = 2$



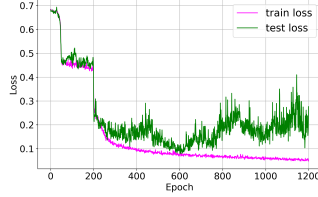
(b) Accuracy curves when $d = 2$



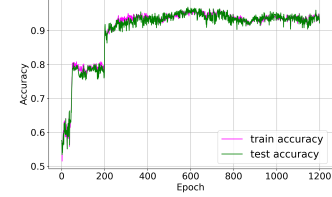
(c) Loss curves when $d = 6$



(d) Accuracy curves when $d = 6$



(e) Loss curves when $d = 8$



(f) Accuracy curves when $d = 8$

Figure 6: Average losses and accuracies at each epoch on synthetic data of different dimensions. The **green** curves denote records on test set, while the **magenta** curves denote records on training set. The turning point of the 1st and 2nd stages is the 200-th epoch.

in Fig.6. When the data is easy to be separated, i.e., it is low-dimensional ($d = 2$), the whole training process does not show much differences between the two training stages in Fig.6a and Fig.6b. As the dimension increases, there are obvious improvements, i.e., the drop of losses and the step-up of accuracies, from the 1st training stage to the 2nd training stage in Fig.6c ~ Fig.6f, at the turning point of 200-th epoch. By progressively training the generators layer by layer, we are able to train the whole complex networks and achieve good performance.

4.2. Performance on Benchmark Data Sets

We train our model on 7 small-scale data sets and 3 large-scale data sets. We randomly pick half of the data as training set, the other half as the test set, except for the data sets of which the training and test sets have already been splitted. After normalizing the data to $[0,1]^d$ in advance by min-max normalization, 20% of the training data are randomly selected as the validation set. During the training process of ML-GRFF, after each epoch, we compute the accuracies of model on validation set. The model that achieves the highest performance simultaneously on training set and validation set will be selected. All the experiments on every data set are repeated 5 times.

Tab.1 and tab.2 illustrate the training and test accuracies of different methods on the small-scale and large-scale data sets respectively. The numbers of training and test set and the dimension of every data set are also listed in the two tables. One can find that in most cases, ML-GRFF outperforms RFF and OPT-RFF a lot and achieves competitive (sometimes even slightly better) results compared with MLP.

4.3. Performance on Image and Robustness

4.3.1. Variant of generative RFF for Image Data

When dealing with image data, we can simply stretch an image of $C \times H \times W$ size, where C, H, W represent the number of channels, height and width respec-

Table 1: Training and test accuracies (%) on small-scale data sets. The highest test accuracies are highlighted in **bold**.

method	dataset (#tr;#te;d)	monks1 (124;432;6)	monks2 (169;432;6)	monks3 (122;432;6)	australia (345;345;14)	climate (270;270;18)	diabetic (576;575;19)	sonar (104;104;60)
RFF	train	95.97 \pm 0.57	91.01 \pm 0.88	97.87 \pm 0.45	94.09 \pm 0.78	100.00 \pm 0.00	80.56 \pm 0.56	100.00 \pm 0.00
	test	79.63 \pm 1.40	74.40 \pm 1.00	92.13 \pm 0.71	85.45 \pm 1.57	92.59 \pm 1.41	69.43 \pm 1.13	75.00 \pm 4.41
OPT-RFF	train	97.26 \pm 1.35	80.95 \pm 2.02	97.21 \pm 0.45	92.93 \pm 1.21	99.78 \pm 0.33	78.47 \pm 0.55	100.00 \pm 0.00
	test	84.91 \pm 1.49	73.01 \pm 1.79	92.96 \pm 0.99	85.10 \pm 2.07	93.93 \pm 1.16	69.04 \pm 1.64	75.96 \pm 4.14
MLP	train	96.94 \pm 0.32	96.80 \pm 1.57	97.05 \pm 0.40	92.93 \pm 2.27	98.37 \pm 0.83	84.27 \pm 3.94	91.35 \pm 5.09
	test	84.31 \pm 1.50	84.86 \pm 2.98	85.37 \pm 1.46	84.64 \pm 1.54	93.26 \pm 1.13	67.97 \pm 1.36	75.77 \pm 2.68
ML-GRFF	train	97.90 \pm 1.50	82.72 \pm 1.96	95.08 \pm 1.56	88.29 \pm 1.74	98.52 \pm 0.70	72.53 \pm 5.45	96.35 \pm 1.76
	test	95.83 \pm 2.15	79.72 \pm 1.18	93.70 \pm 0.99	85.68 \pm 0.95	94.81 \pm 1.22	65.60 \pm 3.20	77.12 \pm 4.23

Table 2: Training and test accuracies (%) on large-scale data sets. The highest test accuracies are highlighted in **bold**.

method	dataset ($\#tr$; $\#te$; d)	adult (32,561; 16,281; 123)	ijcnn (49,990; 91,701; 22)	phishing (5,528; 5,527; 68)
RFF	train	79.09 ± 0.38	95.05 ± 0.21	95.53 ± 0.16
	test	78.83 ± 0.26	92.68 ± 0.15	94.61 ± 0.29
OPT-RFF	train	81.64 ± 0.17	95.46 ± 0.20	95.25 ± 0.26
	test	81.31 ± 0.14	93.30 ± 0.14	94.50 ± 0.41
MLP	train	85.05 ± 0.07	98.58 ± 0.48	97.76 ± 0.50
	test	84.70 ± 0.19	98.54 ± 0.23	95.69 ± 0.23
ML-GRFF	train	85.11 ± 0.24	96.70 ± 0.14	95.51 ± 0.78
	test	84.74 ± 0.06	97.10 ± 0.26	94.33 ± 0.35

tively, to a 1-dimensional vector, then multiple 1-dimensional weight vectors of the same size are generated to build the corresponding GRFF with the image vector. However, such a vectorization operation is equivalent to the full-image convolution in image processing. While current prevailing work tends to convolute the image with very deep layer, small-size kernels, such as vgg [27], resnet [28] and inception [29], which is more efficient in capturing the local features and extracting high-level semantic information in image than full-image convolution. Besides, it is also not practical to include so many $C \times H \times W$ neurons in the output layer of the generator.

Therefore, we design a variant of the generative RFF with multi-layer structure. In this variant, the generators generate small-size, 2-dimensional kernels instead of 1-dimensional weights. Then, in the first layer, we convolute the input images with the kernels. The convoluted images will pass through cosine and sine functions respectively, and the two resulting parts will be concatenated along the dimension of channels, followed by a pooling operation. In the second layer, the same manipulations are performed again on the output of previous layer. After multi-layer operations, including convolution, cosine and sine activation, concatenation and pooling, the final results are stretched to a

1-dimensional vector and an FC layer will predict its label.

4.3.2. *Experiments on Defending Adversarial Attack*

Omitting the generators in the variant of ML-GRFF described above, the model itself will reduce to a CNN with cosine and sine activation functions. The generators actually learn to produce the weights or kernels in every layer of CNN. When inference, by resampling the input noise from \mathbb{P}_0 for many times, the generators in ML-GRFF will keep generating different weights or kernels, which will lead to a specific CNN with cosine and sine activation function every time. Hence, inspired by the randomization and resample mechanism associated with the distribution learning ability of ML-GRFF, we investigate its application in defending the adversarial attack.

Adversarial attack has been a hot topic in studying the robustness of machine learning models. Adding imperceptible perturbations to an image can cause drastically different model performance. Such perturbed images are called adversarial examples. Refer to [30] for a recent detailed review about different approaches in generating adversarial examples and defending attacks.

In this section, we mainly exploit the robustness of ML-GRFF in defending an iterative, gradient-based attack, which is called Iteratively, Least-Likely (Iter.L.L.) attack [31]. [32] proposes a one-step, gradient-based approach, Fast Gradient Sign Method (FGSM), which explains that the cumulative sum of many infinitesimal changes on the high-dimensional input will cause the model to incorrectly response. By taking the gradient of the loss function towards the input and moving the input a small step along the direction of the sign of the gradient, FGSM creates the corresponding adversarial example, which actually linearizes the cost function around the model parameters. Based on the one-step FGSM, to acquire better attack performance, [31] proposes an iterative attack method. The steps for creating adversarial example \mathbf{x}_{adv} of original example \mathbf{x}

in the Iter.L.L. attack can be summarized as follows,

$$\begin{aligned} \mathbf{x}_{\text{adv}}^{(i+1)} &= \text{Clip}_{\mathbf{x}, \epsilon} \{ \mathbf{x}_{\text{adv}}^{(i)} \}, \\ \mathbf{x}_{\text{adv}}^{(i)} &\leftarrow \mathbf{x}_{\text{adv}}^{(i)} - \alpha * \text{sign}(\nabla_{\mathbf{x}} L(\text{model}(\mathbf{x}_{\text{adv}}^{(i)}), y_u; \theta)), \\ \mathbf{x}_{\text{adv}}^{(0)} &= \mathbf{x}. \end{aligned} \quad (14)$$

At i -th iteration, [31] computes the loss between the predicted label with the least-likely label y_u , move the original example a small step α along the direction of the sign of the gradient of the loss with respect to \mathbf{x} , and clip the pixel value of perturbed image to a specific range $[\mathbf{x}_{i,j} - \epsilon, \mathbf{x}_{i,j} + \epsilon]$. [31] sets step length $\alpha = 1$ defaultly. The number of iterations is set as $\min(\epsilon + 4, 1.25\epsilon)$. θ denotes the model parameters and $\text{model}(\cdot)$ denotes the prediction label of the model.

Iter.L.L aims at linearizing the local function around given fixed model parameters. While the generators in ML-GRFF can keep generating different weights or kernels. Hence, we test the ability of ML-GRFF in defending Iter.L.L. attack on MNIST and have the following experiment design.

1. Given an input image \mathbf{x} and a group of noise $\mathbf{N}_{(1)}$ from \mathbb{P}_0 , ML-GRFF can predict its label $\hat{y}_{(0)}$ and compute the loss between the prediction and least-likely label.

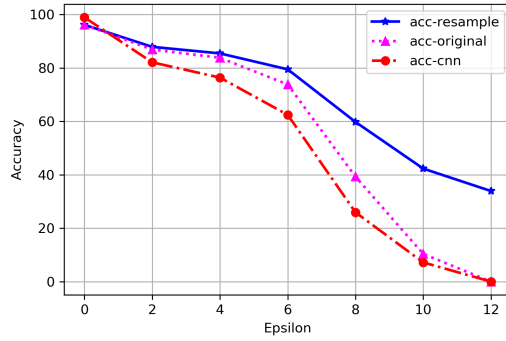


Figure 7: Results of Iter.L.L. attack on ML-GRFF and CNN. The blue solid curve and the magenta dotted curve denote the variations of $\text{acc}_{(2)}$ and $\text{acc}_{(1)}$ with ϵ respectively. While $\text{acc}_{(0)}$ refers to the accuracies at $\epsilon = 0$. The red dashdot curve denotes the variation of attacked accuracies of CNN with cosine and sine activation functions.

2. By back propagation, the gradient of the loss with respect to input \mathbf{x} can be determined.
3. The corresponding adversarial examples \mathbf{x}_{adv} of \mathbf{x} can be build according to Eq.(14).
4. ML-GRFF can take \mathbf{x}_{adv} and original noise $\mathbf{N}_{(1)}$ as input and output a prediction $\hat{y}_{(1)}$.
5. By resampling a new group of noise $\mathbf{N}_{(2)}$ from \mathbb{P}_0 , now ML-GRFF can take \mathbf{x}_{adv} and new noise $\mathbf{N}_{(2)}$ as input and output another prediction $\hat{y}_{(2)}$.

We denote the unattacked accuracy, attacked accuracy with original noise, attacked accuracy with resampled noise as $acc_{(0)}$, $acc_{(1)}$ and $acc_{(2)}$ respectively. It is expected that the attacked accuracies $acc_{(1)}$ and $acc_{(2)}$ should be smaller than $acc_{(0)}$, and that $acc_{(2)}$ should be larger than $acc_{(1)}$ since resampling should be helpful in defending Iter.L.L. attack.

For image data, the generator Φ_G is parameterized the same as the generator in DCGAN [19]. We only change the values of kernel size, padding and stride in the de-convolution operation so that our generator can generate small-size kernels. We also adopt a two-layer architecture, the generators of which generate 16 and 8 kernels of 5×5 size in the 1st and 2nd layer respectively. The max-pooling manipulations take a perception field of 2×2 size. The experiment results are shown in Fig.7. By omitting the generators in ML-GRFF, we acquire a CNN with cosine and sine activation function. We also record the results of Iter.L.L. attack on such a CNN in Fig.7.

One can find that under Iter.L.L. attack, by resampling noise from \mathbb{P}_0 , $acc_{(2)}$ are generally larger than $acc_{(1)}$. When ϵ equals to 12, which means 15 iterations, all the adversarial examples successfully fool CNN and ML-GRFF with original noise and result in zero accuracies. While by resampling a new group of noise, ML-GRFF successfully identifies nearly 40% of these adversarial examples, which is a promising improvement. Besides, both the attacked accuracies with resampled noise and original noise are higher than the attacked accuracy of CNN. Therefore, due to the randomization and resampling mechanism asso-

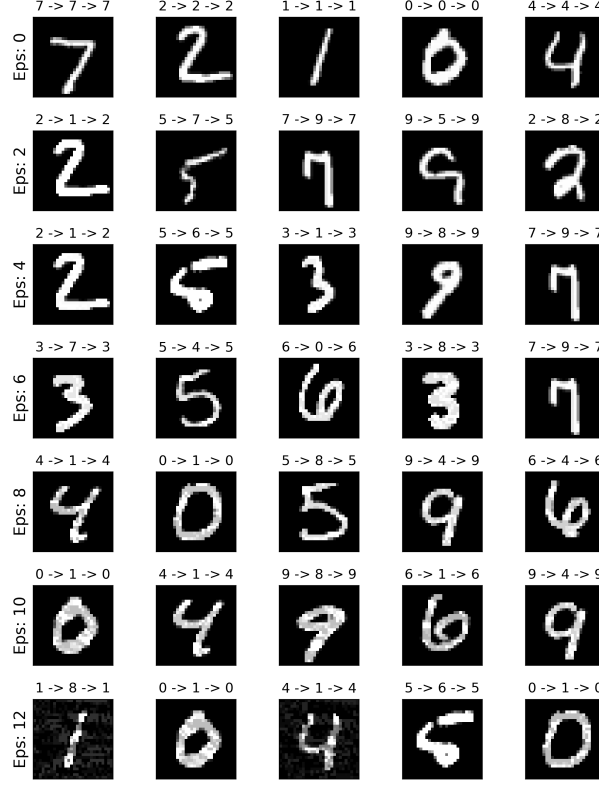


Figure 8: Illustration of some adversarial examples of Iter.L.L attack. Different ϵ values correspond to different rows of adversarial examples. Among the 3 numbers at the top of each adversarial example, the first number denotes the true label, and the middle number denotes prediction $\hat{y}_{(1)}$, and the last number denotes prediction $\hat{y}_{(2)}$. These adversarial examples (except the first row) successfully fool the model without resampling. But the model successfully identifies these adversarial examples by resampling.

ciated with ML-GRFF, our model is able to alleviate the performance decrease brought by Iter.L.L. attack. It also shows superiority over common CNN of the same structure in defending Iter.L.L. attack. Part of the adversarial examples are shown in Fig.8.

5. Discussion and Conclusion

In conclusion, we propose a one-stage kernel learning approach, which models some latent distribution of the kernel with a generative network based on random Fourier features. Not like the existing methods that learn the distribution by kernel alignment and then build a linear classifier, we directly solve the ERM problem to jointly learn the features and classifier for better generalization performance. Further, such an end-to-end manner enables the model itself to extend to deeper layers, which leads to the multi-layer structure and can learn a good kernel on the features. Besides, a progressive training strategy is proposed to efficiently train the multiple generators in different layers in an inverse, layer-by-layer order. Empirical results illustrate the superiority of ML-GRFF in classification tasks over other two-stage, RFF-based methods. Meanwhile, generative RFF enables us to resample different parameters from the generators and keeps stable accuracies. Such randomness of the parameters is helpful in defending adversarial attacks. Empirical results also demonstrate that it is efficient in alleviating the performance decrease brought by adversarial examples.

One of the limitations of the proposed method is that its performance on large-scale image data and deeper network is still restricted. In our method, for image data, the generators try to learn the distributions on the 3×3 or 5×5 kernels. However, in deeper network, like ResNet [28], a usual size of kernels in the convolution layer is $512 \times 512 \times 3 \times 3$. The generator cannot include $512 \times 512 \times 3 \times 3$ neurons in its output layer since it is a heavy burden for GPU to compute the gradients. Besides, more layers require more generators. Training tens of, or even hundreds of generators is still a difficult problem.

Since the parameter distribution is modeled by generative networks, which cost huge memory and computation resources, future work will focus on how to design cheap and efficient mechanism to model the parameter randomness and to achieve better robustness.

Acknowledgment

This research is partly supported by NSFC, China (No.61876107,61977046, U1803261,61806125), Committee of Science and Technology, Shanghai, China (No.19510711200) and National Key Research Development Project (No. 2018AAA0100702). Jie Yang and Xiaolin Huang are the corresponding authors.

References

References

- [1] B. Scholkopf, A. J. Smola, Learning with kernels: support vector machines, regularization, optimization, and beyond, MIT press, 2001.
- [2] M. Filippone, F. Camastra, F. Masulli, S. Rovetta, A survey of kernel and spectral methods for clustering, Pattern recognition 41 (1) (2008) 176–190.
- [3] M. Gönen, E. Alpaydm, Multiple kernel learning algorithms, Journal of machine learning research 12 (Jul) (2011) 2211–2268.
- [4] A. Nazarpour, P. Adibi, Two-stage multiple kernel learning for supervised dimensionality reduction, Pattern Recognition 48 (5) (2015) 1854–1862.
- [5] A. G. Wilson, Z. Hu, R. Salakhutdinov, E. P. Xing, Deep kernel learning, in: Artificial Intelligence and Statistics, 2016, pp. 370–378.
- [6] I. Lauriola, C. Gallicchio, F. Aioli, Enhancing deep neural networks via multiple kernel learning, Pattern Recognition 101 (2020) 107194.
- [7] J. Zhuang, I. W. Tsang, S. C. Hoi, A family of simple non-parametric kernel learning algorithms, Journal of Machine Learning Research 12 (Apr) (2011) 1313–1347.
- [8] A. Rahimi, B. Recht, Random features for large-scale kernel machines, in: Advances in neural information processing systems, 2008, pp. 1177–1184.

- [9] A. Sinha, J. C. Duchi, Learning kernels with random features, in: *Advances In Neural Information Processing Systems*, 2016, pp. 1298–1306.
- [10] C.-L. Li, W.-C. Chang, Y. Mroueh, Y. Yang, B. Póczos, Implicit kernel learning, in: *The 22nd International Conference on Artificial Intelligence and Statistics*, 2019, pp. 2007–2016.
- [11] W. Rudin, *Fourier analysis on groups*, Vol. 121967, Wiley Online Library, 1962.
- [12] N. Cristianini, J. Shawe-Taylor, A. Elisseeff, J. S. Kandola, On kernel-target alignment, in: *Advances in neural information processing systems*, 2002, pp. 367–373.
- [13] M. Mohri, A. Rostamizadeh, A. Talwalkar, *Foundations of machine learning*, MIT press, 2018.
- [14] F. Liu, X. Huang, Y. Chen, J. Yang, J. A. K. Suykens, Random fourier features via fast surrogate leverage weighted sampling, in: *Proceedings of 34th AAAI Conference on Artificial Intelligence (AAAI-20)*, -, 2019.
- [15] W. Zhang, Z. Zhang, L. Wang, H.-C. Chao, Z. Zhou, Extreme learning machines with expectation kernels, *Pattern Recognition* 96 (2019) 106960.
- [16] M. Belkin, D. Hsu, S. Ma, S. Mandal, Reconciling modern machine-learning practice and the classical bias–variance trade-off, *Proceedings of the National Academy of Sciences* 116 (32) (2019) 15849–15854.
- [17] I. Goodfellow, Y. Bengio, A. Courville, *Deep learning*, MIT press, 2016.
- [18] I. Goodfellow, J. Pouget-Abadie, M. Mirza, B. Xu, D. Warde-Farley, S. Ozair, A. Courville, Y. Bengio, Generative adversarial nets, in: *Advances in neural information processing systems*, 2014, pp. 2672–2680.
- [19] A. Radford, L. Metz, S. Chintala, Unsupervised representation learning with deep convolutional generative adversarial networks, in: *International Conference on Learning Representations*, 2016.

- [20] T. Karras, T. Aila, S. Laine, J. Lehtinen, Progressive growing of gans for improved quality, stability, and variation, in: International Conference on Learning Representations, 2018.
- [21] K. Ukai, T. Matsubara, K. Uehara, Hypernetwork-based implicit posterior estimation and model averaging of cnn, in: Asian Conference on Machine Learning, 2018, pp. 176–191.
- [22] N. Ratzlaff, L. Fuxin, Hypergan: A generative model for diverse, performant neural networks, in: International Conference on Machine Learning, 2019, pp. 5361–5369.
- [23] S. Ioffe, C. Szegedy, Batch normalization: Accelerating deep network training by reducing internal covariate shift, in: International Conference on Machine Learning, 2015, pp. 448–456.
- [24] N. Srivastava, G. Hinton, A. Krizhevsky, I. Sutskever, R. Salakhutdinov, Dropout: a simple way to prevent neural networks from overfitting, The journal of machine learning research 15 (1) (2014) 1929–1958.
- [25] D. P. Kingma, J. Ba, Adam: A method for stochastic optimization, in: International Conference on Learning Representations, 2015.
- [26] S. Wold, K. Esbensen, P. Geladi, Principal component analysis, Chemometrics and intelligent laboratory systems 2 (1-3) (1987) 37–52.
- [27] K. Simonyan, A. Zisserman, Very deep convolutional networks for large-scale image recognition, in: International Conference on Learning Representations, 2015.
- [28] K. He, X. Zhang, S. Ren, J. Sun, Deep residual learning for image recognition, in: Proceedings of the IEEE conference on computer vision and pattern recognition, 2016, pp. 770–778.
- [29] C. Szegedy, V. Vanhoucke, S. Ioffe, J. Shlens, Z. Wojna, Rethinking the inception architecture for computer vision, in: Proceedings of the IEEE

conference on computer vision and pattern recognition, 2016, pp. 2818–2826.

- [30] X. Yuan, P. He, Q. Zhu, X. Li, Adversarial examples: Attacks and defenses for deep learning, *IEEE transactions on neural networks and learning systems*.
- [31] A. Kurakin, I. Goodfellow, S. Bengio, Adversarial machine learning at scale, in: *International Conference on Learning Representations*, 2017.
- [32] I. J. Goodfellow, J. Shlens, C. Szegedy, Explaining and harnessing adversarial examples, in: *International Conference on Learning Representations*, 2015.